Serum albumin impedes the amyloid aggregation and hemolysis of human islet amyloid polypeptide and alpha synuclein

Aleksandr Kakinen,[†] Ibrahim Javed,[†] Ava Faridi,[†] Thomas P. Davis[†§] and Pu Chun Ke[†*]*

[†]ARC Centre of Excellence in Convergent Bio-Nano Science and Technology, Monash Institute of Pharmaceutical Sciences, Monash University, 381 Royal Parade, Parkville, VIC 3052, Australia

[§]Department of Chemistry, University of Warwick, Gibbet Hill, Coventry, CV4 7AL, United Kingdom

Corresponding Author

[*] Thomas P. Davis: thomas.p.davis@monash.edu and Pu Chun Ke: pu-chun.ke@monash.edu.

ABSTRACT. Protein aggregation is a ubiquitous phenomenon underpinning the origins of a range of human diseases. The amyloid aggregation of human islet amyloid polypeptide (IAPP) and alpha synuclein (αS), specifically, is a hallmark of type 2 diabetes (T2D) and Parkinson's disease impacting millions of people worldwide. Although IAPP and αS are strongly associated with pancreatic β-cell islets and presynaptic terminals, they have also been found in blood circulation and the gut. While extensive biophysical and biochemical studies have been focused on IAPP and αS interacting with cell membranes or model lipid vesicles, the roles of plasma proteins on the amyloidosis and membrane association of these two major types of amyloid proteins have rarely been examined. Using a thioflavin T kinetic assay, transmission electron microscopy and a hemolysis assay here we show that human serum albumin, the most abundant protein in the plasma, impeded the fibrillization and mitigated membrane damage of both IAPP and αS. This study offers a new insight on the native inhibition of amyloidosis.

TOC GRAPHIC

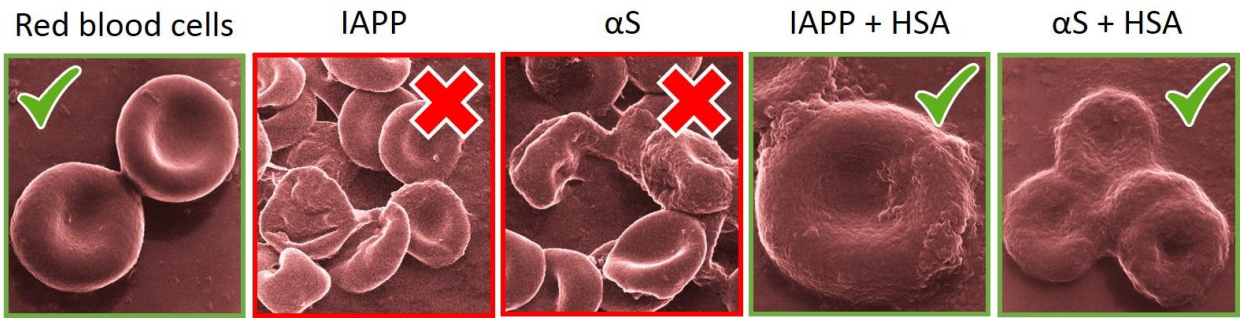

KEYWORDS. Amyloid aggregation · IAPP · αS · protein corona · membrane · inhibition

Introduction

Human islet amyloid polypeptide (IAPP) and alpha synuclein (αS) are two major classes of amyloid proteins serving both functional and pathogenic roles in biology. Specifically, monomeric IAPP assists insulin for glycemic control, while monomeric αS is thought to be associated with the modulation of neurotransmitter dopamine release, endoplasmic reticulum (ER)/Golgi trafficking, and synaptic vesicles [1]. The endogenous stabilization of IAPP is provided by insulin, physiological metal ions, low pH and zinc-mediated complexation of IAPP and C-peptide [2-8]. Likewise, transitions of αS from disordered monomers to partially folded intermediates and amyloid fibrils may be promoted by changes in local pH, ionic strength and temperature, as well as mutation [9, 10].

A large collection of literature has revealed that amphiphilic environments, such as cell membranes and lipid vesicles, can initiate electrostatic interactions between the N-termini of amyloid proteins and the anionic membranes [11-16], facilitated by hydrophobic interaction and hydrogen bonding between the interactants. Such interactions have been shown to convert the proteins from disordered monomers to α-helix and then β-sheet rich oligomers and protofibrils and, eventually, cross-beta amyloid fibrils. The oligomers and amyloid fibrils show a high propensity for partitioning into cell membranes, causing pore formation in a porin-like manner or extracting lipid content to compromise membrane fluidity [17-20]. The endpoints of such interactions range from generation of reactive oxygen species (ROS) to damage to ER, mitochondria, and DNA, followed by cell degeneration. Furthermore, it has been found that the aromatic side chains of LANFLVH, a fragment of IAPP, are nonessential in amyloid formation or membrane leakage [21], while cholesterol showed contrasting effects on IAPP toxicity and disruption to model membranes [22].

In addition, inhibition of IAPP amyloidosis and increased IAPP resistance to protease degradation by copper (II) has also been reported [23].

IAPP amyloid aggregation has been implicated as causative to the onset of type 2 diabetes (T2D). Likewise, the amyloid aggregation of αS into Lewy bodies or Lewy neurites is closely associated with motor symptoms and Parkinson's disease. While IAPP fibrils and plaques are generally found in the extracellular space of pancreatic β-cell islets, Lewy bodies and Lewy neurites are located intracellularly. Regardless, oligomeric IAPP and αS have been widely acknowledged as the toxic species based on *in vitro* and animal studies [24, 25].

IAPP is stored at millimolar concentrations in pancreas beta islets and readily fibrillates at micromolar concentrations [3]. Upon release into the bloodstream, IAPP is immediately exposed to a milieu of plasma proteins and lipids [26, 27]. Consequently, we have recently applied the concept of protein 'corona' [28, 29] originated from the field of nanomedicine for describing the structural transformation as well as the toxicity of IAPP in circulation [27]. Here the protein corona was rendered by model plasma proteins adsorbed on fibrillating IAPP or mature, hydrophobic IAPP fibrils through electrostatic and hydrophobic interactions as well as H-bonding, similarly to the formation of a protein corona adsorbed on nanoparticles [27, 29]. On the other hand, αS has recently been found in the heart and the gut, with the latter being hypothesized as a possible origin of the protein through the propagation of intestinal microbiota [30, 31]. Interestingly, human serum albumin (HSA), which accounts for 55% of all plasma proteins, has recently been found to possess a chaperone-like capacity against the amyloid aggregation of amyloid beta and transthyretin [32-34], and this capacity of HSA was postulated to be realized through a 'monomer-competitor' mechanism for amyloid beta [35]. Accordingly, in the present study we examined the binding of HSA with IAPP and αS, two major types of amyloid proteins with significant health implications.

We evaluated the effects of their binding on the conformation and toxicities of the amyloid proteins using a thioflavin T (ThT, for fibrillization kinetics) assay and high-resolution transmission electron microscopy (TEM, for mesoscopic morphology), as well as a red blood cell (RBC) hemolysis assay (cell association and membrane leakage). Our study revealed a prolonged lag phase of IAPP and suppressed fibrillization of αS with the increase of HSA concentration. Additionally, the hemolysis assay demonstrated a protective effect of HSA on the toxicities of IAPP and αS towards RBCs. Together, these results offered a new perspective on the natural inhibition of IAPP and αS amyloidosis through the mediation of plasma proteins.

Results and discussion

Effects of HSA on IAPP and αS fibrillization

The fibrillization kinetics of IAPP and αS in the presence of different HSA concentrations was examined using the amyloid specific dye ThT (Fig. 1). The lag phase of IAPP (50 μM) fibrillization at 37 ºC was approximately 20 min, followed by an elongation phase and a saturation phase after 2 h of incubation (Fig. 1A). In the presence of 10 μM HSA (5:1 molar ratio of IAPP to HSA) the lag phase was increased considerably to 4.2 h and the elongation phase to 8 h. With the HSA concentration increased to 50 μM (i.e., 1:1 IAPP to HSA molar ratio), the lag time was extended to 5.4 h while the elongation phase up to 11 h. At the highest tested HSA concentration of 100 μM (1:2 IAPP to HSA molar ratio), the lag time was further extended to 9 h while the saturation phase was reached after 13 h. This result demonstrates the deceleration effect of HSA on the fibrillization kinetics of IAPP, which could be due to the attraction between cationic IAPP and negatively charged HSA at physiological pH, or through hydrophobic interaction between the amyloidogenic region of IAPP (i.e. residues 20-29) and the hydrophobic domains of HSA to reduce IAPP availability for nucleation and elongation. This observation is consistent with the

aggregation inhibition of amyloid beta in the presence of HSA at comparable HSA/amyloid protein ratios [35].

Our electron microscopy imaging confirmed the formation of IAPP amyloid fibrils after 17 h for the control (Figs. 2A,B) and for IAPP incubated with HSA (Figs. 2C-H). However, the presence of HSA altered the IAPP fibril morphology. Namely, at IAPP to HSA molar ratio of 5:1 the IAPP amyloid fibrils were stacked together into multi-fibrillar bundles (Figs. 2C,D). At a higher HSA concentration of 50 μM, IAPP fibrillated into large aggregates displaying significant intertwining (Figs. 2E,F). At excess HSA concentration of 100 μM we observed clear co-aggregation of fibrillar IAPP with HSA (Figs. 2G,H).

In addition, our statistical analysis of the TEM images revealed that HSA exerted a concentration-dependent influence on IAPP fibril length and rigidity (Figs. 4A-D). The persistence length (λ), a major indicator of rigidity [36], is 2,885 nm for (control) IAPP fibrils (Fig. 4A), which is comparable to that of beta lactoglobulin and amyloid-beta fibrils [37, 38]. The lowest HSA concentration did not significantly affect the persistence length or contour length of IAPP (Fig. 4B). However, at 1:1 IAPP to HSA molar ratio we noted a three-fold softening of the amyloid fibrils (λ = 846 nm) and a narrower distribution of the fibril contour length (Fig. 4C). It should be acknowledged that the analysis of amyloid aggregates is not straightforward and may result in underestimated fibril contour length. Interestingly, the highest HSA concentration yielded more rigid fibrils (λ = 3,684 nm, or 27% increase from that of the control) (Fig. 4D).

Understandably, the kinetics of αS fibril formation was markedly slower compared to IAPP, partly due to the much larger molecular weight of the neuronal protein (140 residues vs. 37 residues, or 14,460 Da vs. 3,904 Da for αS vs. IAPP) as well as other different physicochemical attributes of

the amyloid proteins (sequence, charge, and hydrophobicity etc.). The lag phase of αS at 50 μM, 37 ºC and with 500 rpm of shaking was up to 60 h, followed by a steep elongation phase up to 125 h (Fig. 1B; Figs. 3A,B). In the presence of the lowest HSA concentration (10 μM, 5:1 IAPP to HSA molar ratio), αS fibrillization was markedly supressed according to the ThT fluorescence intensity, but was not entirely halted according to TEM imaging (Figs. 3C,D). At lower αS to HSA molar ratios (i.e. 1:1 and 1:2), no increase of ThT fluorescence (Fig. 1B) and no fibrils – according to TEM (Figs. 3E-H) – were observed up to 125 h of incubation. Due to the shaking applied to the samples to speed up fibril formation, the contour length analysis yielded relatively short fibrils only (Fig. 4E). The persistence length of αS fibrils was found to be 1,141 ± 9 nm, or 40% that of IAPP fibrils, whereas the presence of HSA increased the fibril persistence length up to 2,771 ± 3 nm (Fig. 4E), comparable to that of IAPP control in the absence of the plasma protein.

It has been proposed that the effect of (external) ligands on protein amyloid aggregation depends on the relative strength between protein-protein binding and protein-ligand binding [39]. In the case of IAPP, electrostatic attraction between IAPP (isoelectric point or pI: 8.9) [40] and HSA (pI: 4.7) at equal molar concentration likely compromised the assembly of β sheets in amyloid fibril formation, resulting in both softer and shorter fibrils (Figs. 2E,F). This electrostatic interaction mediated the bundling of IAPP fibrils at the highest IAPP:HSA molar ratio (Figs. 2C,D), while caused IAPP fibrils to stiffen through the adsorption of an HSA corona at the highest plasma protein concentration (Figs. 2G,H). In the case of αS, HSA adsorption yielded a corona layer at the 5:1 αS:HSA molar ratio (Figs. 3C,D), while at lower αS:HSA molar ratios the repulsion between the like-charged neuronal protein (pI: 4.67) [41] and plasma protein as well as their hydrophobic interactions could interfere with the self-assembly of αS, thereby inhibiting αS fibril formation.

Ex vivo hemolysis of red blood cells

One facile system for screening the toxicity of exogenous substances is the *ex vivo* hemolysis assay [42]. In this assay, the erythrocyte membranes serve as a model system for probing interactions between toxic compounds and the lipid bilayer. This model has been previously adopted to evaluate the endosomolytic behavior of cell-penetrating peptides, pH-responsive endosomolytic agents for cytosolic delivery [43], as well as other polymeric gene delivery systems [42, 44, 45]. Here we applied the hemolysis assay to examine the interactions of red blood cells (RBCs) with IAPP and αS w/o HSA (Fig. 5A). Evidently, both IAPP and αS demonstrated hemolytic activities against RBCs confirming their toxicity. Consistently with the ThT assay and TEM imaging, the hemolysis assay revealed a minor effect induced by the amyloid proteins mixed with HSA of 10 μM (5:1 molar ratio). However, no hemolysis of RBCs was detected at both 1:1 and 1:2 amyloid proteins to HSA molar ratios alluding to the protective effect of the plasma protein. Using helium ion microscopy we observed noticeable damage to RBCs in DI water (Fig. 5B), or when the cells were exposed to IAPP (Fig. 5E), αS (Fig. 5I), or the amyloid proteins mixed with HSA of 10 μM (Figs. 5F,J). In those cases, the RBC cells appeared deformed from their usual biconcave-discoid shape, and at times were fully ruptured. No membrane damage was visible at higher HSA concentrations for either IAPP (Figs. 5G,H) or αS (Figs. 5K,L), while the RBC cell membranes displayed more rugged morphologies than the control likely resulting from HSA adsorption.

Amyloid formation is a complex, multistep process, comprising the lag, elongation and saturation phases. Oligomeric species, formed during the lag process as an intermediate state, are postulated to be the most toxic of amyloidogenic proteins [3], including IAPP and αS. Over the past decade, a number of molecular mechanisms have been proposed for amyloid oligomer toxicity, indicating the complex and dynamic nature of amyloidosis [46]. One of the widely accepted causes of

oligomeric toxicity is excessive formation of ROS during amyloid fibrillization. Despite free radicals are a normal component of cellular oxygen metabolism in mammals, free radical-associated damage is an important factor in many pathological processes, including amyloid diseases. Albumin, on the other hand, has many known physiological functions, including the binding and transport of various endogenous and exogenous substances [47, 48]. Moreover, HSA has been found to be an important circulating antioxidant [49]. Thus, HSA can protect RBCs from hemolysis through its physical interaction with toxic oligomeric species, or its antioxidative property.

Conclusion

This study has generated several key findings concerning the interactions between plasma protein HSA and amyloid proteins IAPP and αS, an important aspect relevant to amyloidosis but has not been examined extensively in the literature. It has been shown that the major plasma protein HSA impeded the fibrillization of IAPP and αS, likely through competitive protein-protein and protein-ligand interactions [39], consistent with the 'monomer-competitor' mechanism proposed for the chaperone-like activity of HSA against the aggregation of amyloid beta [35]. Specifically, HSA displayed a dose-dependent suppression of IAPP fibrillization kinetics, leading to delayed but not diminished amyloid fibril formation. In comparison, HSA completely inhibited the fibrillization of αS up to 125 h, also coupled with the fact that the neuronal protein, much larger in molecular weight but opposite in charge, fibrillates significantly slower than IAPP. In addition, we have found that HSA can protect RBCs from hemolysis incurred by the toxic IAPP and αS, which can be attributed to the protective mechanism of the plasma protein through its physical interaction with RBCs or its antioxidative property.

Materials and Methods

Materials

Human islet amyloid polypeptide (IAPP; 37 residues, 2-7 disulfide bridge, 3,904 Da, >95% pure by HPLC) and α-synuclein (αS; 140 residues, 14,460 Da, >95% pure by SDS-PAGE and mass spectrometry) were obtained in lyophilized monomeric form from AnaSpec, and prepared in Milli-Q water (Millipore) at a stock concentration of 100 μM at room temperature immediately prior to use. Thioflavin T (ThT) dye and human serum albumin (HSA, 66,478 Da, ≥ 97% pure by gel electrophoresis) were both acquired from Sigma-Aldrich.

Thioflavin T (ThT) assay

IAPP and αS fibrillization in the presence or absence of HSA was analyzed by a ThT assay. For this 50 μM ThT dye, 50 μM of IAPP or αS monomers and 10 μM, 50 μM or 100 μM HSA were mixed, and the ThT fluorescence (read from bottom) was measured at 37 °C over 17 h for IAPP and 125 h (500 rpm linear shaking) for αS, using an EnSpire Multimode Plate Reader (Perkin Elmer; excitation/emission: 440 nm/485 nm) and a 96-well plate (Costar black/clear bottom). The ThT kinetic assay was performed in technical triplicate, and average spectra of 3 measurements were analyzed and presented by blank subtraction and normalized by IAPP/αS fluorescence at saturation.

Transmission electron microscopy (TEM) and analysis

IAPP and αS amyloids fibrillated (17 h for IAPP and 125 h for αS) alone or with different ratios with HSA were examined using high-resolution TEM. For this a 5 μL of amyloid-containing

solution was pipetted onto glow discharged (15 s) copper grids (400 mesh; ProSciTech), followed by 1 min of adsorption. Excess samples were then drawn off using filter paper and the grids were washed by Milli-Q water with the excess drawn off. Then the grids were stained with a drop of 1% uranyl acetate for 30 s. The excess stain was drawn off and the grids were air dried. Imaging was performed by a Tecnai G2 F20 transmission electron microscope (FEI) operated at a voltage of 200 kV. Images were recorded using a Gatan UltraScan 1000 (2k×2k) CCD camera (Gatan, California, USA) and Gatan Microscopy Suite control software.

Statistical analysis of amyloid fibrils

The persistence length (λ) and contour length of IAPP and αS fibrils were analyzed using open source tracking and analysis software – FiberApp by a semi-automated fibril tracking procedure based on the A* pathfinding algorithm (minimal-cost path calculation or Dijkstra's method) (Fig. 4H) [36]. The persistence length reflects an intrinsic property of a polymer, denoting its rigidity and is mathematically defined by the bond correlation function (BCF) in 3D or 2D as the length over which angular correlations in the tangential direction decrease by a factor of *e* (Fig. 4G). Here the λ values of IAPP and αS fibrils were estimated using the average values derived from three methods: BCF, mean-squared end-to-end distance (MSED) and mean-squared midpoint displacement (MSMD). The contour length of a polymer corresponds to the end-to-end length along its contour/backbone (Fig. 4G). Statistical analysis was performed by tracking 97~336 fibrils in multiple TEM images per sample condition (Figs. 4A-F, n value).

Ex vivo hemolysis assay

IAPP, αS and their mixtures with HSA at different molar ratios were subjected to a hemolysis assay to assess the toxicities of the amyloid proteins to RBCs. Blood was collected from a healthy human donor after obtaining informed consent in accordance with the University of Melbourne

Human ethics approval 1443420 and the Australian National Health and Medical Research Council Statement on Ethical Conduct in Human Research. The freshly drawn blood was centrifuged at 2 *g* for 5 min and RBCs were collected as pellets. The RBCs were washed three times with Dulbecco phosphate buffer saline (PBS) by centrifugal washings and diluted up to 5× with PBS. 100 μL of RBCs were incubated with 100 μL of each sample. The final sample concentration after mixing with RBCs was 50 μM for IAPP and αS, and 10 μM, 50 μM and 100 μM for HSA. Samples containing αS, IAPP and their mixtures with HSA were pre-incubated in water for 2 days (500 rpm linear shaking) and 1 h at 37 °C, respectively, and mixed with PBS of 1× in final concentration. After mixing with RBCs, the samples were incubated for 2 h at 37 ºC, centrifuged at 2 *g* for 5 min to pellet down the non-lysed RBCs, and hemolysis was measured by analyzing the absorbance of free hemoglobin leaked out of compromised RBCs in the supernatants at 541 nm (EnSpire Multimode Plate Reader, PerkinElmer). The RBCs incubated with PBS and 50% water (1:1 cells in PBS with Milli-Q water) were used as 0% and 100% hemolysis controls. The percentage hemolysis was determined as:

$$Hemolysis(\%) = \frac{Ab_t - Ab_0}{Ab_{100} - Ab_t} \times bt \,, \tag{1}$$

where Ab_t, Ab_0 and Ab_{100} are absorbance values of the sample, the negative and the positive control, respectively. The hemolysis assay was performed in technical triplicate and average values of 3 measurements were analyzed and presented.

Helium ion microscopy

RBCs treated by IAPP, αS and their combinations with HSA at different molar ratios were incubated overnight with 2.5% paraformaldehyde at 4 ºC and subsequently washed with gradient

concentrations of ethanol, i.e., 20%, 40%, 60%, 80% and 100%, with 2 h incubation at each gradient. A drop of RBCs in 100% ethanol was placed on a carbon tape and the sample morphologies were visualized by helium ion microscopy (Orion NanoFab, Zeiss, USA).

ACKNOWLEDGMENT

This work was supported by ARC Project CE140100036 (Davis). Davis is thankful for the award of an ARC Australian Laureate Fellowship.

Author contributions

P.C.K. and T.P.D. conceived the project. A.K. performed TEM imaging and statistical analysis. A.K. and A.F. carried out the ThT assay. I.J., A.K. and A.F. performed the hemolysis assay and helium ion microscopy. A.K. and P.C.K. wrote the manuscript.

Conflicts of interest

The authors declare no conflict of interest.

REFERENCES

[1] M. Vilar, H.T. Chou, T. Lührs, S.K. Maji, D. Riek-Loher, R. Verel, G. Manning, H. Stahlberg, R. Riek, The fold of α-synuclein fibrils, Proc. Natl. Acad. Sci. USA, 105 (2008) 8637-8642.

[2] L. Haataja, T. Gurlo, C.J. Huang, P.C. Butler, Islet amyloid in type 2 diabetes, and the toxic oligomer hypothesis, Endocr. Rev., 29 (2008) 303-316.

[3] P.C. Ke, M.A. Sani, F. Ding, A. Kakinen, I. Javed, F. Separovic, T.P. Davis, R. Mezzenga, Implications of peptide assemblies in amyloid diseases, Chem. Soc. Rev., 46 (2017) 6492-6531.

[4] J.R. Brender, K. Hartman, R.P.R. Nanga, N. Popovych, R. de la Salud Bea, S. Vivekanandan, E.N.G. Marsh, A. Ramamoorthy, Role of zinc in human islet amyloid polypeptide aggregation, J. Am. Chem. Soc., 132 (2010) 8973-8983.

[5] R.P.R. Nanga, J.R. Brender, S. Vivekanandan, A. Ramamoorthy, Structure and membrane orientation of IAPP in its natively amidated form at physiological pH in a membrane environment, Biochim. Biophys. Acta, 1808 (2011) 2337-2342.

[6] J.L. Larson, A.D. Miranker, The mechanism of insulin action on islet amyloid polypeptide fiber formation, J. Mol. Biol., 335 (2004) 221-231.

[7] M.F. Sciacca, D. Milardi, G.M. Messina, G. Marletta, J.R. Brender, A. Ramamoorthy, C. La Rosa, Cations as switches of amyloid-mediated membrane disruption mechanisms: calcium and IAPP, Biophys. J., 104 (2013) 173-184.

[8] X. Ge, A. Kakinen, E.N. Gurzov, W. Yang, L. Pang, E.H. Pilkington, P. Govindan-Nedumpully, P. Chen, F. Separovic, T.P. Davis, P.C. Ke, F. Ding, Zinc-coordination and C-peptide complexation: a potential mechanism for the endogenous inhibition of IAPP aggregation, Chem. Commun., 53 (2017) 9394-9397.

[9] R. Khurana, C. Ionescu-Zanetti, M. Pope, J. Li, L. Nielson, M. Ramírez-Alvarado, L. Regan, A.L. Fink, S.A. Carter, A general model for amyloid fibril assembly based on morphological studies using atomic force microscopy, Biophys. J., 85 (2003) 1135-1144.

[10] L. Xu, B. Ma, R. Nussinov, D. Thompson, Familial mutations may switch conformational preferences in α-synuclein fibrils, ACS Chem. Neurosci., 8 (2017) 837-849.

[11] P. Cao, A. Abedini, H. Wang, L.-H. Tu, X. Zhang, A.M. Schmidt, D.P. Raleigh, Islet amyloid polypeptide toxicity and membrane interactions, Proc. Natl. Acad. Sci. USA, 110 (2013) 19279-19284.

[12] Y. Porat, S. Kolusheva, R. Jelinek, E. Gazit, The human islet amyloid polypeptide forms transient membrane-active prefibrillar assemblies, Biochemistry, 42 (2003) 10971-10977.

[13] M. Duan, J. Fan, S. Huo, Conformations of islet amyloid polypeptide monomers in a membrane environment: implications for fibril formation, PLOS ONE, 7 (2012) e47150.

[14] C. Guo, S. Côté, N. Mousseau, G. Wei, Distinct helix propensities and membrane interactions of human and rat IAPP 1–19 monomers in anionic lipid bilayers, J. Phys. Chem. B, 119 (2015) 3366-3376.

[15] D.H.J. Lopes, A. Meister, A. Gohlke, A. Hauser, A. Blume, R. Winter, Mechanism of islet amyloid polypeptide fibrillation at lipid interfaces studied by infrared reflection absorption spectroscopy, Biophys. J., 93 (2007) 3132-3141.

[16] S.M. Patil, S. Xu, S.R. Sheftic, A.T. Alexandrescu, Dynamic α-helix structure of micelle-bound human amylin, J. Biol. Chem., 284 (2009) 11982-11991.

[17] R.A. Ritzel, J.J. Meier, C.-Y. Lin, J.D. Veldhuis, P.C. Butler, Human islet amyloid polypeptide oligomers disrupt cell coupling, induce apoptosis, and impair insulin secretion in isolated human islets, Diabetes, 56 (2007) 65-71.

[18] M. Gao, R. Winter, The effects of lipid membranes, crowding and osmolytes on the aggregation, and fibrillation propensity of human IAPP, J. Diabetes. Res., 2015 (2015) 21.

[19] Y. Hirakura, W.W. Yiu, A. Yamamoto, B.L. Kagan, Amyloid peptide channels: blockade by zinc and inhibition by Congo red (amyloid channel block), Amyloid, 7 (2000) 194-199.

[20] R. Kayed, Y. Sokolov, B. Edmonds, T.M. McIntire, S.C. Milton, J.E. Hall, C.G. Glabe, Permeabilization of lipid bilayers is a common conformation-dependent activity of soluble amyloid oligomers in protein misfolding diseases, J. Biol. Chem., 279 (2004) 46363-46366.

[21] D. Milardi, M.F. Sciacca, M. Pappalardo, D.M. Grasso, C. La Rosa, The role of aromatic side-chains in amyloid growth and membrane interaction of the islet amyloid polypeptide fragment LANFLVH, Eur. Biophys. J., 40 (2011) 1-12.

[22] M.F. Sciacca, F. Lolicato, G. Di Mauro, D. Milardi, L. D'Urso, C. Satriano, A. Ramamoorthy, C. La Rosa, The role of cholesterol in driving IAPP-membrane interactions, Biophys. J., 111 (2016) 140-151.

[23] A. Sinopoli, A. Magri, D. Milardi, M. Pappalardo, P. Pucci, A. Flagiello, J.J. Titman, V.G. Nicoletti, G. Caruso, G. Pappalardo, G. Grasso, The role of copper(II) in the aggregation of human amylin, Metallomics, 6 (2014) 1841-1852.

[24] S. Zraika, R.L. Hull, C.B. Verchere, A. Clark, K.J. Potter, P.E. Fraser, D.P. Raleigh, S.E. Kahn, Toxic oligomers and islet beta cell death: guilty by association or convicted by circumstantial evidence? Diabetologia, 53 (2010) 1046-1056.

[25] T.P.J. Knowles, M. Vendruscolo, C.M. Dobson, The amyloid state and its association with protein misfolding diseases, Nat. Rev. Mol. Cell. Biol., 15 (2014) 384-396.

[26] Y. Xing, E.H. Pilkington, M. Wang, C.J. Nowell, A. Kakinen, Y. Sun, B. Wang, T.P. Davis, F. Ding, P.C. Ke, Lysophosphatidylcholine modulates the aggregation of human islet amyloid polypeptide, Phys. Chem. Chem. Phys., 19 (2017) 30627-30635.

[27] E.H. Pilkington, Y. Xing, B. Wang, A. Kakinen, M. Wang, T.P. Davis, F. Ding, P.C. Ke, Effects of protein corona on IAPP amyloid aggregation, fibril remodelling, and cytotoxicity, Sci. Rep., 7 (2017) 2455.

[28] T. Cedervall, I. Lynch, S. Lindman, T. Berggård, E. Thulin, H. Nilsson, K.A. Dawson, S. Linse, Understanding the nanoparticle–protein corona using methods to quantify exchange rates and affinities of proteins for nanoparticles, Proc. Natl. Acad. Sci. USA, 104 (2007) 2050-2055.

[29] P. Ke, S. Lin, W. Parak, T. Davis, F. Caruso, A decade of the protein corona, ACS Nano, 11 (2017) 11773–11776.

[30] T.R. Sampson, J.W. Debelius, T. Thron, S. Janssen, G.G. Shastri, Z.E. Ilhan, C. Challis, C.E. Schretter, S. Rocha, V. Gradinaru, M.-F. Chesselet, A. Keshavarzian, K.M. Shannon, R. Krajmalnik-Brown, P. Wittung-Stafshede, R. Knight, S.K. Mazmanian, Gut microbiota

regulate motor deficits and neuroinflammation in a model of Parkinson's disease, Cell, 167 (2016) 1469-1480.

[31] H. Malkki, Could gut microbiota influence severity of Parkinson disease?, Nat. Rev. Neurol., 13 (2016) 66.

[32] M. Algamal, J. Milojevic, N. Jafari, W. Zhang, G. Melacini, Mapping the interactions between the Alzheimer's Ab-peptide and human serum albumin beyond domain resolution, Biophys. J., 105 (2013) 1700-1709.

[33] T.E. Finn, A.C. Nunez, M. Sunde, S.B. Easterbrook-Smith, Serum albumin prevents protein aggregation and amyloid formation and retains chaperone-like activity in the presence of physiological ligands, J. Biol. Chem., 287 (2012) 21530-21540.

[34] M. Algamal, R. Ahmed, N. Jafari, B. Ahsan, J. Ortega, G. Melacini, Atomic-resolution map of the interactions between an amyloid inhibitor protein and amyloid beta (Aβ) peptides in the monomer and protofibril states, J. Biol. Chem., DOI: 10.1074/jbc.M117.792853.

[35] J. Milojevic, A. Raditsis, G. Melacini, Human serum albumin inhibits Aβ fibrillization through a “monomer-competitor” mechanism, Biophys. J., 97 (2009) 2585-2594.

[36] I. Usov, R. Mezzenga, FiberApp: an open-source software for tracking and analyzing polymers, filaments, biomacromolecules, and fibrous objects, Macromolecules, 48 (2015) 1269-1280.

[37] A. Kakinen, J. Adamcik, B. Wang, X. Ge, R. Mezzenga, T. Davis, F. Ding, P. Ke, Nanoscale inhibition of polymorphic and ambidextrous IAPP amyloid aggregation with small molecules, Nano Res., DOI: 10.1007/s12274-017-1930-7.

[38] J. Adamcik, J.-M. Jung, J. Flakowski, P. De Los Rios, G. Dietler, R. Mezzenga, Understanding amyloid aggregation by statistical analysis of atomic force microscopy images, Nat. Nanotech., 5 (2010) 423.

[39] A. Gladytz, B. Abel, H.J. Risselada, Gold‐induced fibril growth: the mechanism of surface‐facilitated amyloid aggregation, Angew. Chem. Int. Ed., 55 (2016) 11242-11246.

[40] S. Li, M. Micic, J. Orbulescu, J.D. Whyte, R.M. Leblanc, Human islet amyloid polypeptide at the air–aqueous interface: a Langmuir monolayer approach, J. Royal Soc. Interface., 9 (2012) 3118-3128.

[41] N. Gould, D.E. Mor, R. Lightfoot, K. Malkus, B. Giasson, H. Ischiropoulos, Evidence of native α-synuclein conformers in the human brain, J. Biol. Chem., 289 (2014) 7929-7934.

[42] K. Saar, M. Lindgren, M. Hansen, E. Eiríksdóttir, Y. Jiang, K. Rosenthal-Aizman, M. Sassian, Ü. Langel, Cell-penetrating peptides: a comparative membrane toxicity study, Anal. Biochem., 345 (2005) 55-65.

[43] B.C. Evans, C.E. Nelson, S.S. Yu, K.R. Beavers, A.J. Kim, H. Li, H.M. Nelson, T.D. Giorgio, C.L. Duvall, *Ex Vivo* red blood cell hemolysis assay for the evaluation of pH-responsive endosomolytic agents for cytosolic delivery of biomacromolecular drugs, J. Vis. Exp., (2013) 50166.

[44] A. Kichler, C. Leborgne, E. Coeytaux, O. Danos, Polyethylenimine-mediated gene delivery: a mechanistic study, J. Gene. Med., 3 (2001) 135-144.

[45] M.F. Sohail, H.S. Sarwar, I. Javed, A. Nadhman, S.Z. Hussain, H. Saeed, A. Raza, N. Irfan Bukhari, I. Hussain, G. Shahnaz, Cell to rodent: toxicological profiling of folate grafted thiomer enveloped nanoliposomes, Toxicol. Res., 6 (2017) 814-821.

[46] R. Kayed, C. Lasagna-Reeves, Molecular mechanisms of amyloid oligomers toxicity, J. Alzheimers Dis., 33 (2013) S67-S78.

[47] U. Kragh-Hansen, V.T.G. Chuang, M. Otagiri, Practical aspects of the ligand-binding and enzymatic properties of human serum albumin, Biol. Pharm. Bull., 25 (2002) 695-704.

[48] B. Carlo, D. Enrico, Reversible and covalent binding of drugs to human serum albumin: methodological approaches and physiological relevance, Curr. Med. Chem., 9 (2002) 1463-1481.

[49] M. Roche, P. Rondeau, N.R. Singh, E. Tarnus, E. Bourdon, The antioxidant properties of serum albumin, FEBS Lett., 582 (2008) 1783-1787.

FIGURES AND CAPTIONS

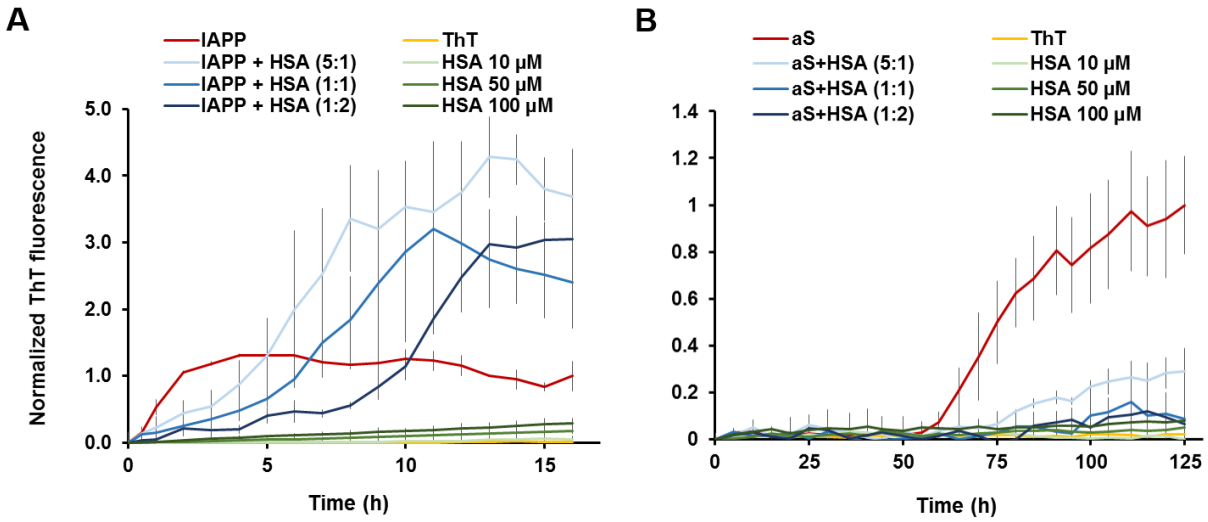

Figure 1. Effects of human serum albumin (HSA) on the fibrillization kinetics of (A) IAPP (50 µM) and (B) αS (50 µM). IAPP fibrillization in presence of 10 µM (5:1 IAPP to HSA molar ratio), 50 µM (1:1) and 100 µM (1:2) of HSA revealed a prolonged lag phase with the increase of HSA concentration. Fibrillization of αS was observed w/o the presence of HSA and with 10 µM (5:1 molar ratio) of HSA. However, αS amyloid formation was inhibited in the presence of higher HSA concentrations (50 µM, 100 µM).

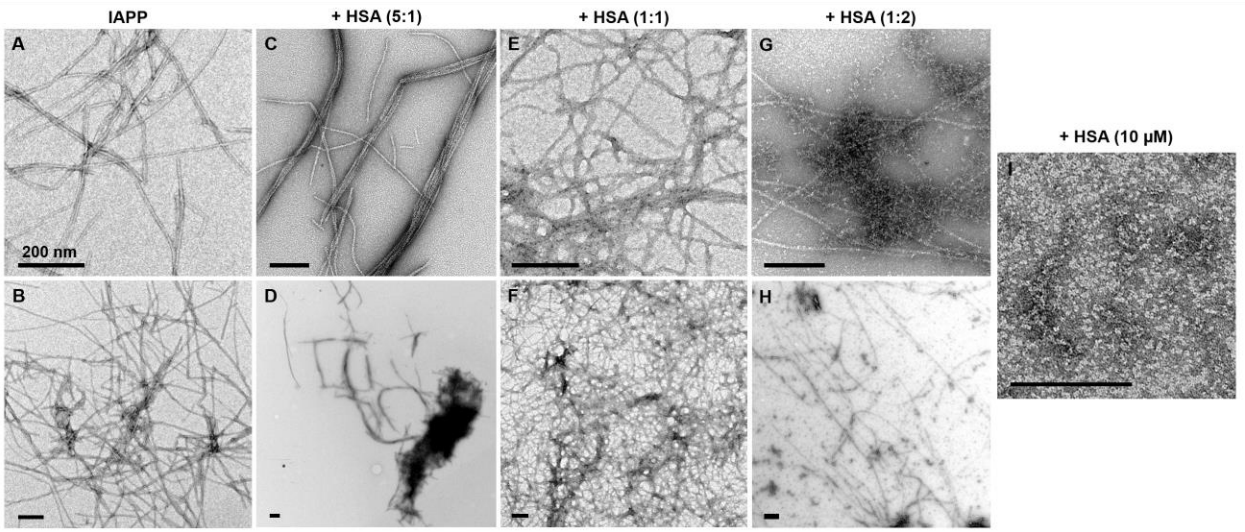

Figure 2. Transmission electron microscopy imaging of IAPP fibrillization w/o and with HSA. (A, B) IAPP fibrils, (C, D) IAPP fibrillized with 10 μM HSA (5:1 IAPP to HSA molar ratio, 17 h incubation), (E, F) 50 μM HSA (1:1 ratio), and (G, H) 100 μM HSA (1:2 ratio). (I) 10 μM HSA (equal to the concentration in the 5:1 ratio case). Scale bars: 200 nm.

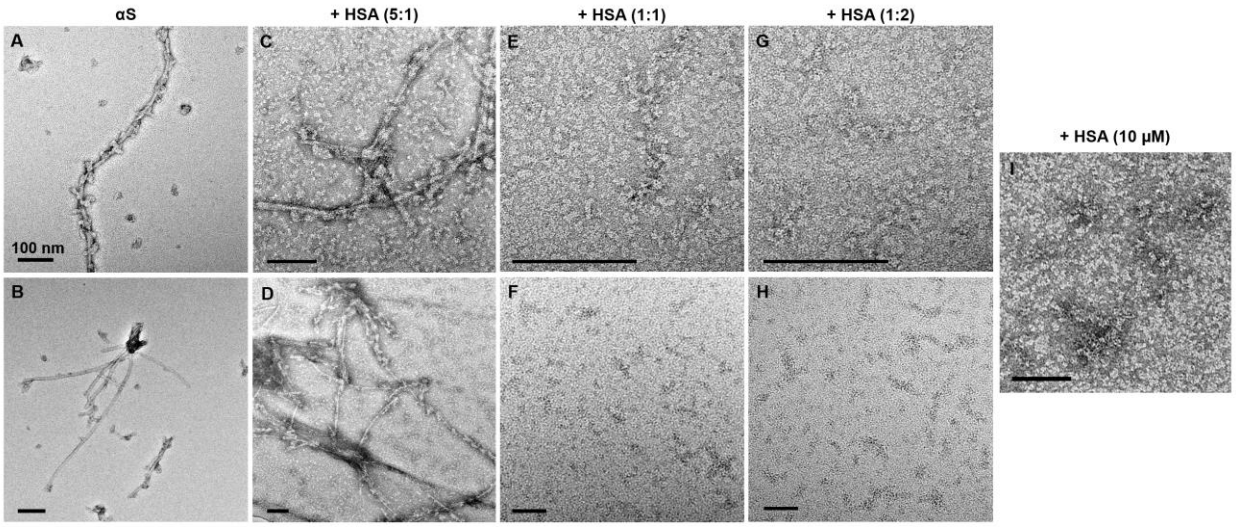

Figure 3. Transmission electron microscopy imaging of αS amyloid fibril formation w/o and with HSA (A, B) αS control, (C, D) αS in the presence of 10 μM HSA, (E, F) αS in the presence of 50 μM HSA, and (G, H) 100 μM HSA. (I) 10 μM HSA (equal to the concentration in the 5:1 ratio case). Scale bars: 100 nm.

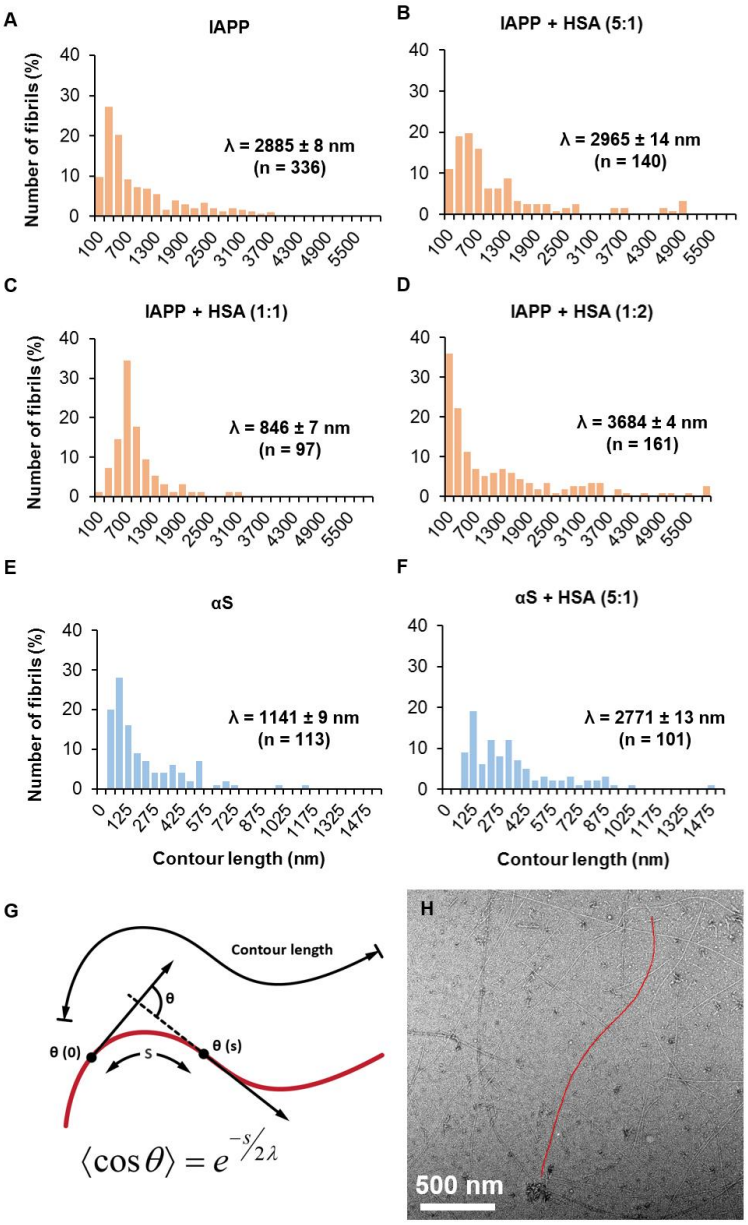

Figure 4. Contour length and persistence length (λ) analyses of IAPP (50 µM) (A-D) and αS (50 µM) (E-F) fibrils incubated with 10 µM (5:1 ratio), 50 µM (1:1 ratio) and 100 µM (1:2 ratio) HSA. The contour length of αS with HSA at 50 µM and 100 µM was not analyzed due to the lack of fibril formation. n: number of analyzed fibrils. (G) Schematic definitions of contour length and persistence length (λ) of the fibril. λ is defined as the length over which angular correlations in the tangent direction decrease by *e* times. Factor 2 in the formula accounts for 2D Euclidean geometry. Contour length corresponds to the end-to-end length of a fibril along its contour. (H) TEM image of IAPP amyloid fibrils and a tracked fibril contour, shown as a red line, by the FiberApp software.

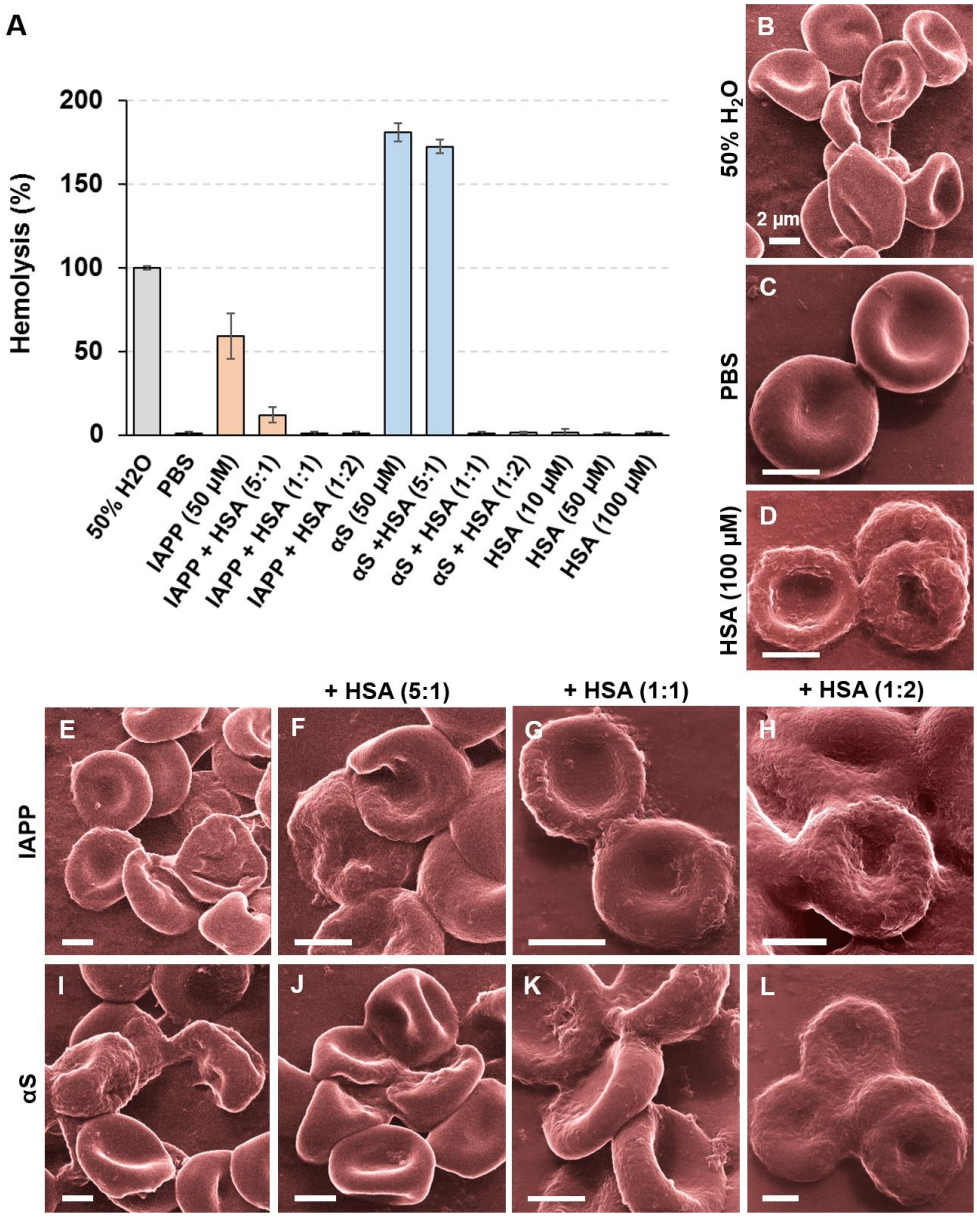

Figure 5. (A) Determination of the *in vitro* toxicities of IAPP, αS and their combinations with HSA against red blood cells (RBCs) with an absorbance-based hemolysis assay. (B-L) Visualization of RBCs damaged by hemolysis using helium ion microscopy. Scale bars: 2 µm.